Research Article

Journal of Labelled Compounds and Radiopharmaceuticals

Received 5 June 2014, Revised 28 July 2014, Accepted 8 August 2014 Published online 25 September 2014 in Wiley Online Library

(wileyonlinelibrary.com) DOI: 10.1002/jlcr.3233

A novel radiochemical approach to 1-(2′-deoxy-2′-[18F]fluoro-β-D-arabinofuranosyl) cytosine (18F-FAC)†

Jan-Philip Meyer,[a,b] Katrin C. Probst,[b] Iuni M. L. Trist,[a] Christopher McGuigan,[a] and Andrew D. Westwell[a]*

^{18}F-FAC (1-(2′-deoxy-2′-[^{18}F]fluoro-β-D-arabinofuranosyl)-cytosine) is an important 2′-fluoro-nucleoside-based positron emission tomography (PET) tracer that has been used for *in vivo* prediction of response to the widely used cancer chemotherapy drug gemcitabine. Previously reported synthetic routes to ^{18}F-FAC have relied on early introduction of the ^{18}F radiolabel prior to attachment to protected cytosine base. Considering the ^{18}F radiochemical half-life (110 min) and the technical challenges of multi-step syntheses on PET radiochemistry modular systems, late-stage radiofluorination is preferred for reproducible and reliable radiosynthesis with *in vivo* applications. Herein, we report the first late-stage radiosynthesis of ^{18}F-FAC. Cytidine derivatives with leaving groups at the 2′-position are particularly prone to undergo anhydro side-product formation upon heating because of their electron density at the 2-carbonyl pyrimidone oxygen. Our rationally developed fluorination precursor showed an improved reactivity-to-stability ratio at elevated temperatures. ^{18}F-FAC was obtained in radiochemical yields of 4.3–5.5% (n = 8, decay-corrected from end of bombardment), with purities ≥98% and specific activities ≥63 GBq/μmol. The synthesis time was 168 min.

Keywords: nucleosides; positron emission tomography; radiochemistry; radiopharmaceuticals; computational chemistry

Introduction

Nucleoside derivatives represent an important emerging class of biomarkers for positron emission tomography (PET) imaging.[1] For example, the clinically approved proliferation biomarker ^{18}F-FLT (3′-deoxy-3′-[^{18}F]fluoro-L-thymidine) is accessible via an effective radiochemical synthesis in high radiochemical yield and purity suitable for human production under Good Manufacturing Practice guidelines.[2] Hence, ^{18}F-FLT is now commonly used for the early detection of various cancers and the evaluation of treatment response.[3] Especially in high-grade tumours, it appears to be more powerful in predicting treatment response and survival than ^{18}F-FDG, as measured by standard uptake values of ^{18}F-FLT directly corresponding to cell proliferation shown by the Ki-67 proliferation index.[4]

Cytidine-based radiotracers for PET imaging such as ^{18}F-FAC (**1**, Figure 1) and 1-(2′-deoxy-2′-[^{18}F]fluoroarabinofuranosyl)-5-methylcytosine (^{18}F-FMAC, **2**, Figure 1) have been previously shown to be successful as predictors of response for nucleoside analogue-based treatment of cancer[5,6] as well as local immune activation in mouse models.[7] As such, ^{18}F-FAC has been used for response prediction to the widely used chemotherapy drug gemcitabine.[5] Gemcitabine is frequently used for (combination) chemotherapy of a number of solid tumours such as pancreatic, non-small cell lung, breast and bladder cancer. Importantly, gemcitabine efficacy is compromised by poor cellular uptake by nucleoside transporters, variable activity of the essential deoxycytidine kinase (dCK) activating enzyme and rapid deactivating metabolism by cytidine deaminase (CDA). In addition, serious dose-limiting toxicities are associated with this chemotherapy drug.[8] Prediction of patient response to gemcitabine chemotherapy would therefore be an important milestone towards personalized patient chemotherapy in the cancer clinic.

Given the close structural resemblance to gemcitabine, ^{18}F-FAC was found to have a comparably high affinity for deoxycytidine kinase (dCK), a rate-limiting enzyme in the nucleoside salvage pathway. Hence, *in vivo* imaging determined dCK-positive and dCK-negative tumours. Furthermore, an additional study showed that ^{18}F-FMAC PET imaging provides information about cytidine deaminase (CDA) enzymatic activity *in vivo*, which is related to gemcitabine resistance.[6] Together, cytidine-based PET probes enable further conclusions towards personalized

[a]*School of Pharmacy and Pharmaceutical Sciences, Cardiff University, Redwood Building, King Edward VII Avenue, Cardiff, CF10 3NB, Wales, UK*

[b]*Wales Research & Diagnostic PET Imaging Centre (PETIC), Institute for Translation, Innovation, Methodology & Engagement (TIME), School of Medicine, Cardiff University, Heath Park, Cardiff, CF14 4XN, Wales, UK*

**Correspondence to: Andrew D. Westwell, School of Pharmacy and Pharmaceutical Sciences, Cardiff University, Redwood Building, King Edward VII Avenue, Cardiff, CF10 3NB, Wales, UK.*
E-mail: WestwellA@cf.ac.uk

†*Additional supporting information may be found in the online version of this article at the publisher's web-site.*

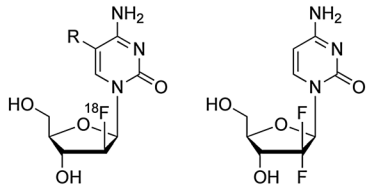

Figure 1. Chemical structures of the cytidine-based biomarkers ^{18}F-FAC, ^{18}F-FMAC and ^{18}F-FIAC (**1–3**), and the anticancer drug gemcitabine.

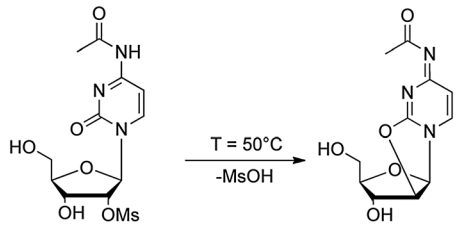

5 **12**

Scheme 1. Heat-mediated intramolecular cyclization towards **12** in d_6-DMSO.

chemotherapy that, considering the low (≤20%) response rates and severe side effects, could lead to significantly improved treatment efficacy.[8]

2′-[^{18}F]arabinocytidines such as ^{18}F-FAC and ^{18}F-FIAC (**3**, Figure 1) have been synthesized in high purities using an early stage ^{18}F introduction strategy.[9] However, this synthetic approach limits reliable and reproducible production on commercially available synthesis modules for human application.[10] For instance, multiple steps after ^{18}F introduction with an additional purification step due to the formation of the D- and L-isomers, as well as the use of toxic substances such as hydrogen bromide, make the translation to automated synthesizers difficult. These challenges go hand in hand with reproducibility issues when it comes to quality control in clinical practice according to the British/European/American Pharmacopeia. Furthermore, as the number and space in hot cells is limited, multiple-step radiosyntheses should preferably be replaced by shorter and less complex synthetic procedures. Lazari *et al.* recently presented a newly designed radiosynthesis module system that furnished the nucleoside analogues ^{18}F-FMAU and ^{18}F-FAC in good overall radiochemical yields (46% and 31%, respectively, decay-corrected) and with acceptable reproducibility following early stage fluoride introduction.[11] Overall synthesis times were reported to be 165–170 min in each case. The flexible radiosynthesizers developed are described as being suitable for both the development and production of different radiotracers for applications in PET.

The aim of this study was to develop a novel and straightforward synthetic approach towards ^{18}F-FAC that could be applied to the radiosynthesis of related cytidine-based radiotracers. A more straightforward radiosynthesis similar to the ^{18}F-FDG synthesis in combination with innovative radiosynthesizers would enable a faster transition from tracer development to clinical application. Late-stage ^{18}F-introduction at the 2′-arabino position of an intact nucleoside towards nucleoside-based radiotracers was previously considered as difficult.[12] However, Alauddin and co-workers recently developed a novel radiosynthesis of the uridine analogue ^{18}F-FMAU based on a late-stage ^{18}F-introduction approach in order to increase possibilities for making nucleoside-based PET tracer suitable for clinical applications.[10,12] The key towards a stable precursor that would be less likely to undergo anhydro side-product formation (e.g. Scheme 1) due to neighbouring group participation was the introduction of a good electron-withdrawing N-protecting group(s). Because the amino group at the 4-position of cytidine derivatives likely enhances the nucleophilicity of the 2-carbonyl oxygen, potential precursor molecules containing a leaving group at the 2′-position are even more prone to undergo anhydro formation especially at high temperatures (≥75 °C). Thus, a reasonable radiofluorination precursor must combine sufficient reactivity with stability towards heat as well as basic conditions. In this study, we present for the first time a late-stage radiofluorination approach to the ^{18}F-labelled cytidine derivative ^{18}F-FAC.

Experimental section

Radiosynthetic procedures

*N^4-bis-Boc-3′,5′-O-bis-tetrahydropyranyl-2′-deoxy-2′-[^{18}F] fluoroarabinocytidine (**25**)*

[^{18}F]fluoride was trapped on a QMA cartridge (equilibrated with 5% $NaHCO_3$ solution (5 mL) and water (5 mL)) before it was eluted with an aqueous solution (0.7 mL) of $KHCO_3$ (22.6 mg/mL) and kryptofix K_{222} (22.6 mg/mL) in MeCN. The resulting ^{18}F/$KHCO_3$/K_{222}-complex was dried by co-evaporation under reduced pressure and a stream of nitrogen. The drying process was repeated three times (3 × 1 mL MeCN). A solution of precursor (**23**) (10 mg, 14.5 μmol) in DMF (0.3 mL) was then added, and the resulting mixture was stirred at 110 °C for 20 min. The crude mixture was either analysed directly for determination of ^{18}F-incorporation (radio-TLC) or passed through an Alumina-Sep-Pak cartridge (equilibrated with water (5 mL)) for characterization (radio-HPLC). The ^{18}F-labelled intermediate was eluted with EtOAc (2 mL), and an aliquot (0.2 mL) of the mixture was analysed by analytical HPLC using co-elution with the non-radioactive reference compound (**24**). R_t = 17.2 min, MeCN/H_2O 9:1, 1 mL/min, ≥87%, radio-TLC, R_f = 0.6 (4% MeOH/DCM).

*^{18}F-FAC (**1**)*

After elution of the ^{18}F-labelled intermediate (**25**) with EtOAc into a new reaction V-vial, the solvent was removed under reduced pressure and a stream of nitrogen at 80 °C. 2N HCl solution (0.3 mL) was added to the dried residue followed by stirring at 90 °C for 15 min. The solution was then neutralized with 2N NaOH solution (0.3 mL). The resulting mixture was loaded onto a semi-preparative HPLC column via a 10-mL injection loop. The fraction containing ^{18}F-FAC was collected after 22.5 min with 3% MeCN in H_2O and a flow rate of 3.5 mL/min. The appropriate fraction was flushed through a sterile filter and concentrated via evaporation on the module (100 °C under a stream of nitrogen for 10 min). The residue was taken up in sterile saline. An aliquot (0.2 mL) of the mixture was analysed by analytical HPLC using co-elution with the non-radioactive reference compound **27**, R_t = 13.8 min, 3% MeCN/H_2O, 1 mL/min, ≥98%. A carrier-added synthesis was performed according to the previous procedure, and the product ^{19}F/^{18}F-FAC was saved for decay for 20 half-lives (≈2 days) and subsequently analysed by mass spectrometry; MS (70 eV): *m/z* (%): 245.4 (5) [$(M+H)^+$], 267.7 (95) [$(M+Na)^+$].

Computational methods

MOE 2010.10 software was used to design each compound and to explore possible conformations. The searching method applied was LowModMD that generates conformations using a short run of molecular dynamics at constant temperature followed by an all-atom energy minimization. Amongst the conformations, 16 of them were selected for each compound for quantum mechanics (QM) evaluation. QM calculations were executed for the selected conformations with the GAMESS[13] software. A geometry optimization was performed *in vacuo*, using analytical energy gradients with the restricted Hartree–Fock wave function. The 3-21G split valence basis set was used, and diffuse sp shell was added to heavy atoms. The initial hessian was guessed, and the convergence gradient tolerance was set to 0.0005 E_h/bohr. The electrostatic potential was calculated at points determined by Michael Connolly algorithm on the surface of van der Waals fused spheres. Atomic charges were consequently fitted to this potential. The partial net charges of atoms of interest were gathered from each molecule conformation, and values were averaged.

Results and discussion

Precursor design

In order to develop a new precursor for radiofluorination of the 2′-arabino position of cytidine derivatives, the idea of radiofluorination of an intact nucleoside moiety was applied. The main challenge of this new approach is the rational design of precursors that combine reactivity and stability in a way that the ^{18}F-nucleophile can be incorporated at high temperatures resulting in acceptable conversion rates whilst heat-mediated anhydro formation is kept to a minimum. A quantitative method for the characterization of precursor stabilities was desirable prior to synthesis. The electric charge density of the 2-carbonyl oxygen of the pyrimidone moiety was determined using theoretical methods for the potential to undergo an intramolecular nucleophilic attack at the 2′-position. Hence, the net electric charge of the 2-carbonyl oxygen of a family containing N^4-substituted cytidine derivatives (**4–8**, Figure 2) was calculated using quantum chemical calculations with restricted Hartree–Fock wave function and the 3-21G basis set.

Additionally, selected uridine derivatives (**9–11**, Figure 2) were included in this study, in order to obtain both a reference value as well as a measurement of how the substitution of the 4-carbonyl group (uridines) by an amino group (cytidines) impacts the electric charge density at the 2-carbonyl oxygen. The N-substituents were chosen with regard to both their synthetic accessibility and deprotection mechanisms that would be suitable for radiochemical syntheses in terms of subsequent efficient removal. The N^3-nitro-2′-(methanesulfonyl)uridine (**11**) was considered as a standard value as a N^3-nitro-2′-(trifluoromethanesulfonyl) uridine derivative was previously reported as successfully synthesized and thermal stable.[14] However, the radiofluorination method could not be applied to a N^3-nitro-uridine-based precursor.

The results shown later (Table 1) indicate that the electron density at the 2-carbonyl oxygen is reduced when H-substitution at the N^4 (N^3 for uridine derivatives) with an electron-withdrawing group is performed. Furthermore, it shows that the stronger the electron-withdrawing effect of the substituent(s), the lower the calculated electron density Ω at the 2-carbonyl oxygen. For instance, double N^4-Boc-protection (**7**) decreases the electron density more than single N^4-Boc-protection (**6**) and N^4-monoacetylation (**5**), respectively.

Compounds **5** and **7** were synthesized (see Synthesis section and Supporting information) and subsequently tested for their ability to undergo heat-mediated decomposition by forming the appropriate anhydro compounds **12** and **13**. First, an NMR sample of compound **5** in d_6-DMSO was heated up to 50 °C. ^{1}H-NMR spectra were recorded hourly. Figure 3 shows that almost full conversion to anhydro compound **12** occurred after 2 h (Scheme 1).

Chemical shifts of the amino proton (11.5 to 12.25 ppm) and the ribose protons clearly show the conversion into the cyclic nucleoside compound (Figure 3). Furthermore, the vanishing signal of the mesyl group at 3.5 ppm also indicates decomposition as the free mesylate is expected to have a different chemical shift that indeed could be observed at around 2.3 ppm next to the methyl-signal of the acetamide. ^{13}C-NMR data after 1-h incubation showed 24 instead of 12 signals of pure compound **5**. Additionally, ESI-MS was performed in order to show the change in the molecular mass. The *m/z*-signal 268 $[M+H]^+$ further confirmed generation of anhydro compound **12**.

The double N^4-Boc-protected compound (**7**), however, showed significantly increased thermal stability as shown in Scheme 2 and Figure 4. Even though a tiny set of additional

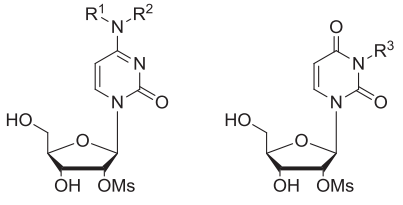

4 $R^1 = R^2 = H$
5 $R^1 = H$, $R^2 = Ac$
6 $R^1 = H$, $R^2 = Boc$
7 $R^1 = R^2 = Boc$
8 $R^1 = R^2 =$ phthalimide

9 $R^3 = H$
10 $R^3 = Boc$
11 $R^3 = NO_2$

Figure 2. Selected cytidine-based and uridine-based nucleosides for electric charge density calculations at 2-carbonyl oxygen.

Table 1. Calculated electron density Ω of selected cytidine (**4–8**) and uridine derivatives (**9–11**)

No.	R^1	R^2	R^3	$[\Omega \pm \%]^a$
4	H	H		−0.911 ± 0.09
5	H	Ac		−0.901 ± 0.05
6	H	Boc		−0.860 ± 0.01
7	Boc	Boc		−0.825 ± 0.06
8	Phthalimide	Phthalimide		−0.814 ± 0.08
9			H	−0.838 ± 0.02
10			Boc	−0.770 ± 0.03
11			NO_2	−0.589 ± 0.10

[a]Quantum chemically calculated net charge at the 2-carbonyl oxygen.

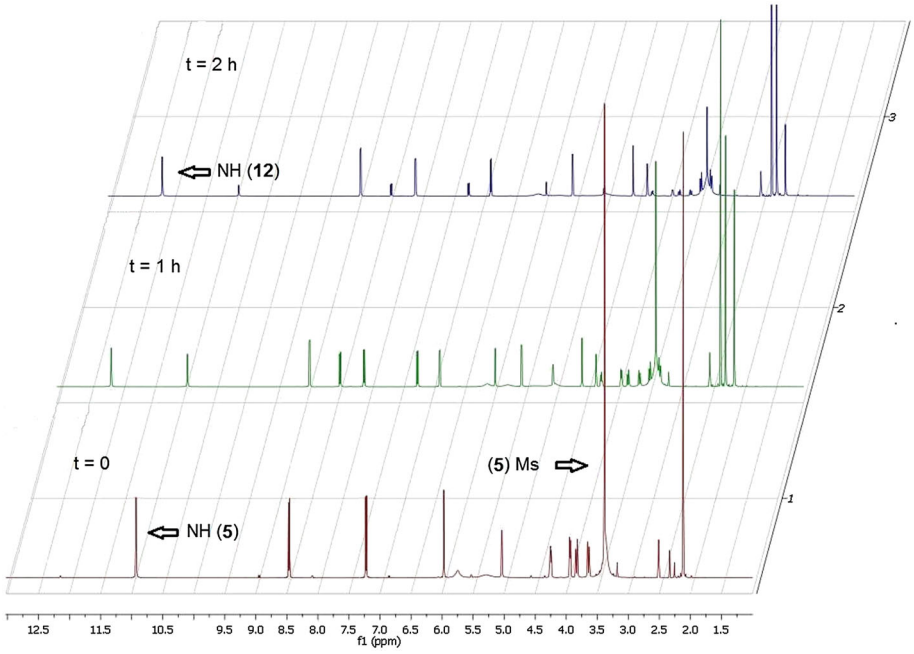

Figure 3. Heat-mediated anhydro formation of **12**. After only 2 h at 50 °C, nearly full conversion could be observed by ^{1}H NMR analysis.

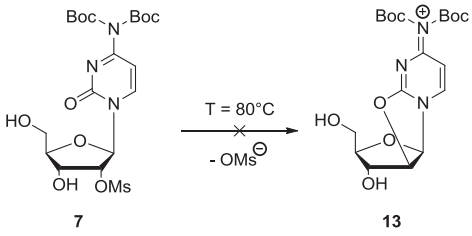

Scheme 2. Increased thermal stability of **7**. No significant formation of side product (**13**) could be observed (in d_4-MeOD).

peaks appeared after 2 h at 80 °C, the observed stability of compound **7** looked promising with regard to ^{18}F-radiolabelling reactions.

Hence, the calculated and experimental data lead to three major conclusions: (1.) The electron density at the 2-carbonyl oxygen of the pyrimidine moiety can be used as a measurement for its ability to undergo intramolecular cyclization resulting in the appropriate 2,2′-anhydro compounds. (2.) Electron-withdrawing groups have a measurable/quantifiable effect on the electron density at the 2-carbonyl oxygen. (3.) Depending on the strength of its electron-withdrawing nature, a N^4(N^3)-protecting

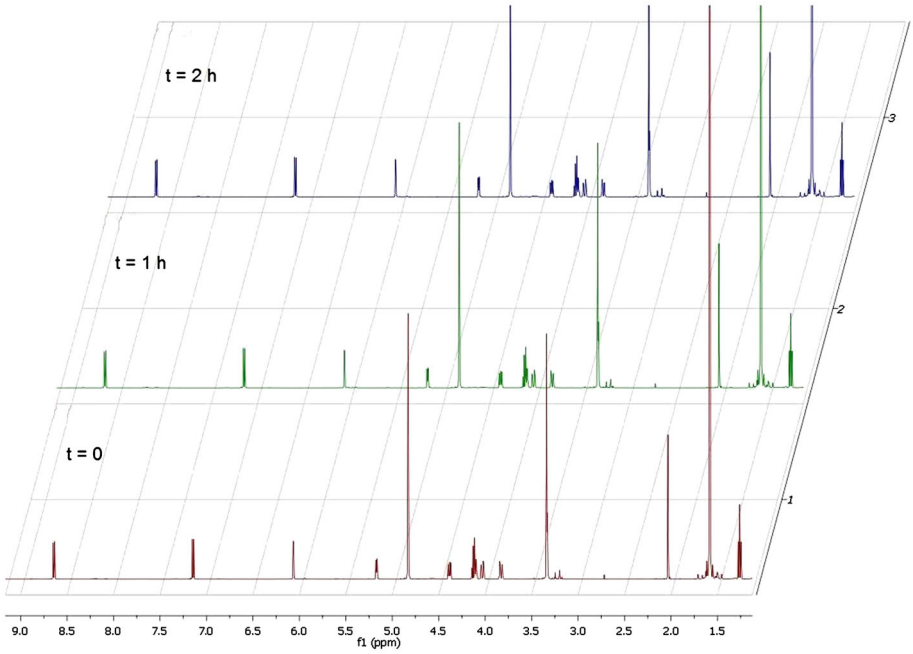

Figure 4. Recorded ^{1}H-NMR spectra of purified compound (**7**) after 0, 60 and 120 min at 80 °C. The absence of additional peaks indicate no or minimal anhydro formation through increased thermal stability.

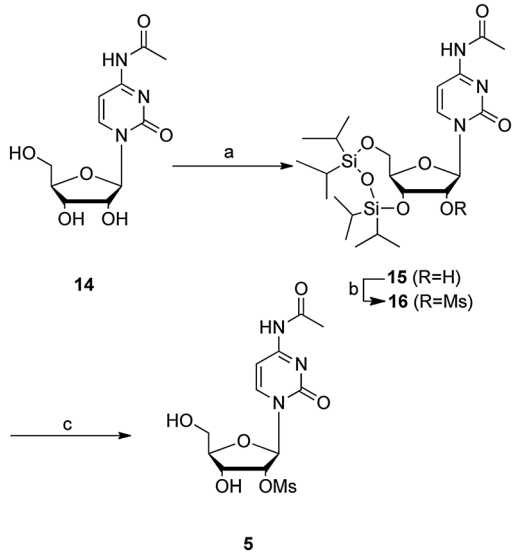

Scheme 3. Reagents and conditions: (a) $TIPDSCl_2$, pyridine, 0 °C – room temperature (RT), 12 h, 87%; (b) MsCl, TEA, DCM, 0 °C – RT, 2 h, 81%; (c) TBAF, THF, −10 °C, 30 min, 53%.

group influences the thermal stability of the nucleoside analogue. Finally, an N,N-diBoc fluorination precursor was selected for radiofluorination studies.

Synthesis

The synthesis of test compound **5** was carried out with the selective 3′- and 5′-protection of *N*-acetylcytidine (**14**) using $TIPDSCl_2$ in pyridine yielding compound **15** in good yield, which was consecutively mesylated at the 2′-position using an excess of MsCl and TEA in DCM furnishing compound **16**. Subsequent removal of the silica-based protecting group using TBAF in anhydrous THF at low temperatures gave test compound **5** that was purified immediately and characterized because of its high ability to undergo anhydro formation (Scheme 3).

The synthesis of precursor (**23**) started with commercially available cytidine (**17**), which was first converted into the 3′- and 5′-protected nucleoside **18** using $TIPDSCl_2$ and pyridine at room temperature as previously described.[8] Subsequent TMS-protection furnished **19** that was followed by double N^4-Boc-protection using excess of Boc_2O (5–6 eq.) and DMAP that gave compound **20** in good yield. Selective removal of the TMS-group using *p*-TsOH was performed at −5 °C to give intermediate **21**. Subsequent mesylation of the free 2′-hydroxy group was performed in high yield to form compound **22**. TBAF-mediated removal of the bidentate-protecting group had to be carried out at lower temperatures (approximately −10 °C) in order to avoid significant decrease in yield probably because of single Boc-group removal. Purified compound **7** was then converted into fluorination precursor **23** using 3,4-dihydro-6H-pyran in excess. Highly purified precursor **23** was obtained in 9% overall yield from **17** (Scheme 4).

The choice of the leaving group as well as the protecting group is based on a previous study[10] that found that 3′/5′-THP protection of uridine derivatives gave the best radiochemical yields and a 2′-mesyl group an appropriate balance between stability and leaving group abilities. Furthermore, our pilot studies showed that the appropriate tosyl-containing and nosyl-containing counterparts already decomposed during purification. Furthermore, even though double THP protection makes NMR analysis complex (mixture of diastereomers), the later removal of these groups was straightforward.

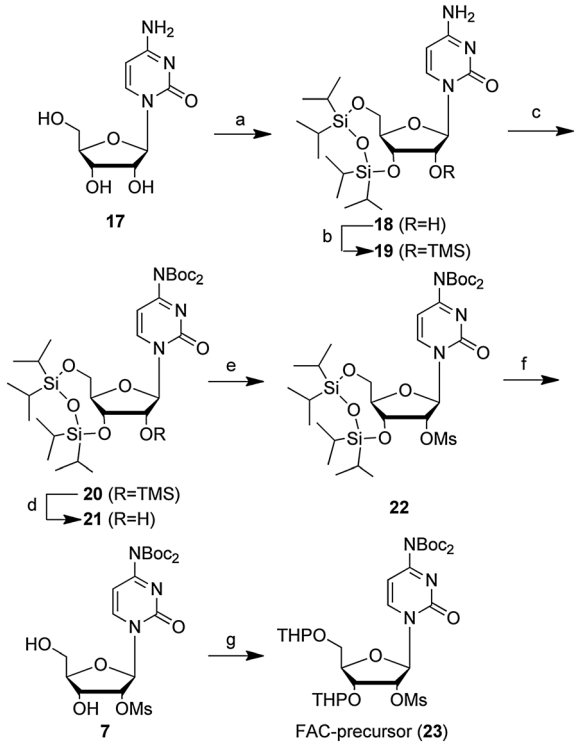

Scheme 4. Reaction conditions: (a) $TIPDSCl_2$, pyridine, 0 °C – RT, 18 h, 81%; (b) TMSCl, TEA, DCM, 0 °C – RT, 2 h, 83%; (c) Boc_2O, DMAP, DCM, RT, 5 h, 77%; (d) *p*-TsOH, THF, −5 °C, 66–78%; (e) MsCl, TEA, DCM, 0 °C, 90%; (f) TBAF, THF, −10 °C, 70–80%; and (g) DHP, pTsOH, DCM, 0 °C – RT, 6–8 h, 45–56%.

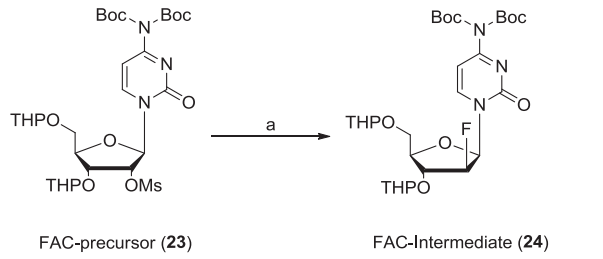

Scheme 5. Reagents and conditions: (a) 1N TBAF/THF, DMF, 100 °C, 100 min, 19%.

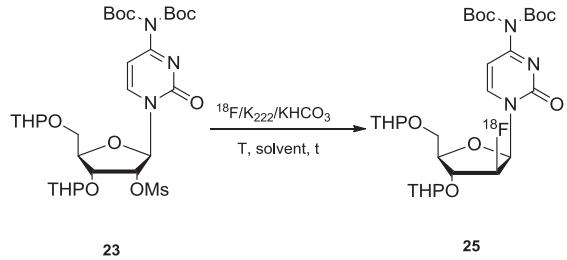

Scheme 6. Radiofluorination was performed using different reaction conditions as outlined in the table later.

Firstly, cold fluorination reactions were carried out to assess fluoride incorporation for precursor (**23**). Amongst fluorination conditions tested, the best incorporation yield was found at 100 °C for 100 min in DMF using freshly prepared 1N TBAF/THF-solution (Scheme 5). The fluorinated intermediate (**24**) was purified by column chromatography on SiO_2, and its identity and purity (≥97%) confirmed by $^{1}H/^{19}F$-NMR, HR-MS and analytical HPLC (Supporting information). Notably, the ^{19}F-spectrum showed a set of four signals due to the four diastereomers that the THP protection yields.

The obtained intermediate **24** was used as a cold reference standard for co-elution on HPLC in order to identify the hot intermediate.

Radiosynthesis of ^{18}F-FAC

The ^{18}F-incorporation to form intermediate (**25**) was carried out using an Eckert & Ziegler modular system and appropriate software for radiosynthesis. The reaction parameters of solvent, temperature and reaction time were varied in order to determine optimal ^{18}F-incorporation conditions, using $KHCO_3$ as base (Scheme 6). [^{18}F]Fluoride was eluted from the QMA cartridge using a $K_{222}/KHCO_3$ solution. Table 2 shows the calculated incorporation data, and Figure 5 shows ^{18}F-incorporation plotted against the reaction temperature run in dry DMF as solvent. The highest incorporation values were obtained using DMF at 110 °C for 20 min. Although MeCN or *t*BuOH as solvent failed to show any conversion, the use of an alternative base such as TBA–OH or TBA–CO_3 in MeCN or *t*BuOH might provide an alternative strategy. However, higher temperatures and longer reaction times led to decreased ^{18}F-incorporation in the arabino position because of the formation of the anhydro intermediate. ^{18}F-incorporation was calculated by peak integration of the crude reaction mixture after radiofluorination using radio-TLC (Supporting information).

The ^{18}F-fluorinated intermediate (**25**) was confirmed by radio-HPLC (Figure 6) and co-injection of the ^{19}F-containing reference standard (**24**) (Supporting information) after trapping the majority of the unreacted ^{18}F-fluoride on a Sep-Pak alumina cartridge. The intermediate was eluted with 2.5 mL EtOAc into a new reaction vial.

The solvent was then removed at 90 °C under a stream of nitrogen. 2N HCl solution was added to the dried residue (**25**), which was then stirred at 95 °C for 20 min (Scheme 7). A shorter deprotection time was found to lead to decreased final yields of the product ^{18}F-FAC.

After neutralization with 2N NaOH solution, the mixture was loaded onto a semi-preparative HPLC column via a 10-mL injection loop. [^{18}F]-FAC was eluted after 22.5 min at a flow rate of 3.5 mL/min using 3% MeCN in H_2O as the mobile phase. Following concentration on the module (100 °C

Table 2. [^{18}F]-incorporation results obtained under different conditions

No.	Solvent	T [°C]	t [min]	[^{18}F][a] [%]
1	MeCN	90	20	n/a
2	*t*BuOH	95	20	n/a
3	DMF	90	20	1.3 ± 0.3
4	DMF	95	20	2.6 ± 0.2
5	DMF	100	20	4.9 ± 0.6
6	DMF	105	20	7.7 ± 0.8
7	DMF	110	20	9.4 ± 0.8
8	DMF	110	30	7.9 ± 0.6
9	DMF	115	20	6.9 ± 0.5
10	DMF	120	20	4.1 ± 0.4
11	DMF	125	20	2.3 ± 0.2
12	DMF	130	20	1.8 ± 0.2

[a][^{18}F]-incorporation was calculated using radio-TLC. Each reaction was repeated three times under identical conditions.

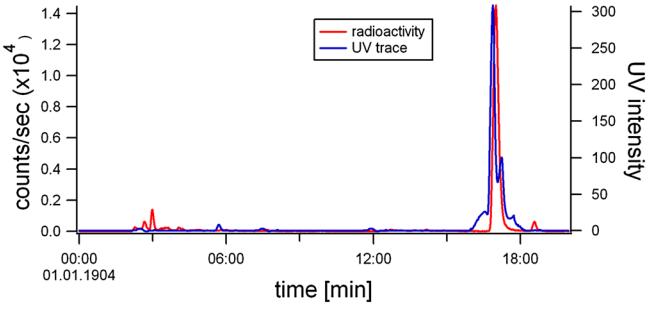

Figure 6. Radio-HPLC was performed in order to confirm the formation of **25**. The fluoridation product was co-eluted with reference compound **24** after 17.2 min (MeCN/H_2O 10:1, flow rate of 1 mL/min). The profile of the radio-HPLC diagram is consistent with the radio-TLC diagram shown earlier.

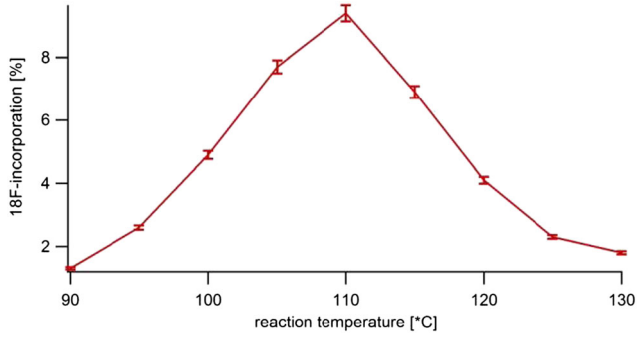

Figure 5. [^{18}F]-incorporation plotted against the reaction temperature run in dry DMF as solvent.

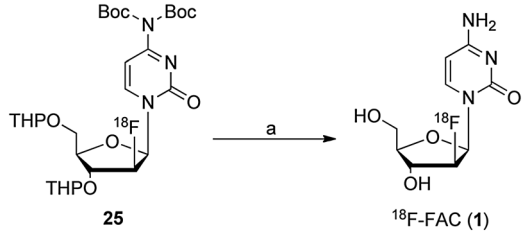

Scheme 7. Subsequent deprotection of the hot intermediate **25** using (a) 2N HCl at 95 °C for 20 min. A shorter deprotection time results in decreased final yields of the product ^{18}F-FAC (**1**).

under a stream of nitrogen for 10 min), the sample was taken up in sterile saline, and an aliquot was co-eluted on an analytical HPLC in combination with both possible 2′-^{19}F-isomers FC (**26**) and FAC (**27**) as references (Figures 7 and 8). ^{18}F-FAC was confirmed, and its purity calculated to ≥98% with specific activity of ≥63 GBq/μmol. The total synthesis time was 168 min, including the concentration and saline formulation time. Finally, 0.75–0.86 GBq of ^{18}F-FAC was obtained resulting in radiochemical yields of 4.3–5.5% (n = 8, decay-corrected from end of bombardment).

Additionally, a temperature study was performed to reveal why the ^{18}F-incorporation decreases when the reaction temperature is increased. According to the mechanism, intramolecular anhydro formation is expected at higher temperatures leading to a lower yield of the correct stereoisomer. Figure 9 shows radio-HPLC traces that were recorded after radiofluorination at

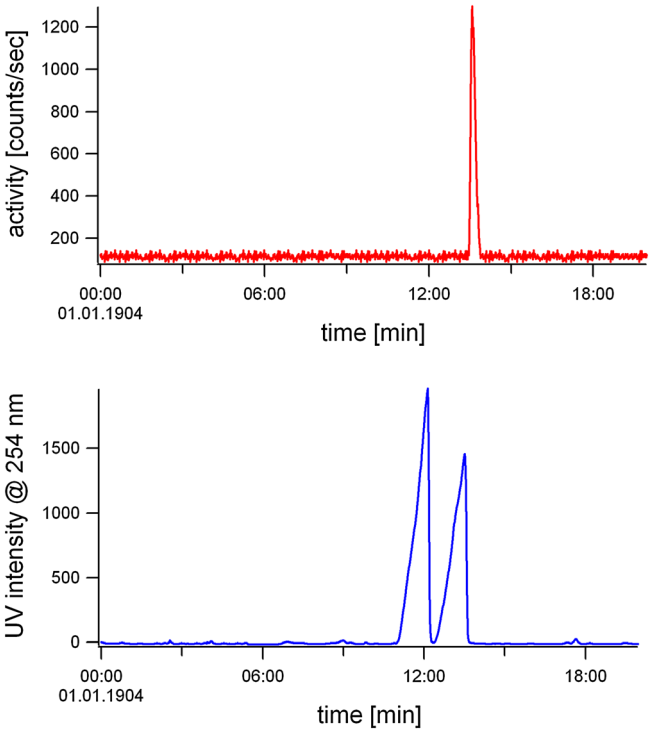

Figure 7. Radio-HPLC chromatogram of the purified fraction. Co-elution with both cold 2′-[^{19}F]-isomers **26** and **27** confirms that the correct stereoisomer was obtained.

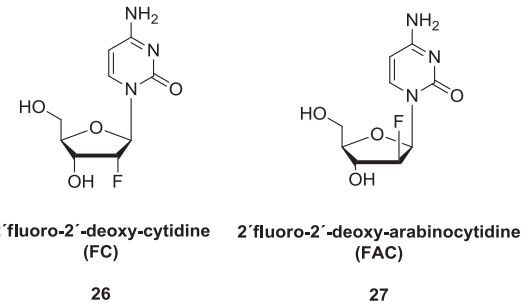

Figure 8. Chemical structures of the two different 'cold' 2′-fluoro-cytidines FC (**26**) and FAC (**27**).

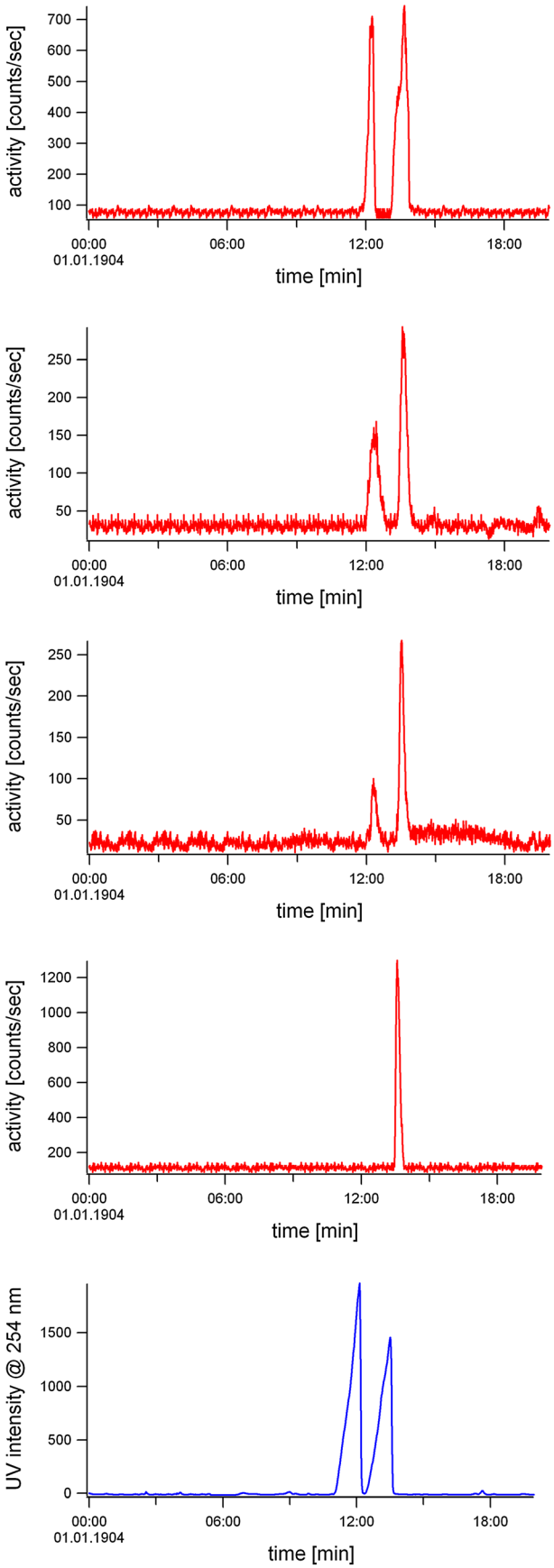

Figure 9. Radio-HPLC traces recorded after radiofluorinations performed at different reaction temperatures.

110, 120 and 130 °C (20 and 40 min, bottom to top panel respectively) and co-elution with both 2′-fluoro stereoisomers FC and FAC (bottom panel). The results show that higher temperatures do lead to anhydro formation and radiofluorination of the anhydro intermediate results in ^{18}F-FC. The ^{18}F-FAC/FC ratio decreases as the reaction temperature and time increase.

Conclusions

A novel radiochemical approach to ^{18}F-FAC is described. For the first time, ^{18}F-FAC was synthesized via late-stage radiofluorination of the intact pyrimidine nucleoside. Prior to synthesis, a novel fluorination precursor was designed using *in silico* methods and stability studies monitored by NMR. Precursor **23** was found to be a promising candidate for further testing out of the family of nucleosides that were investigated. ^{18}F-incorporation studies led to optimal reaction conditions (110 °C, 20 min) that furnished ^{18}F-FAC in 4.3–5.5% decay-corrected radiochemical yield. Considering that this new process involves late-stage fluorination and labelling of a cytidine derivative (more challenging than the equivalent uridine derivative), our radiochemical yield is good. Our overall synthesis time (168 min) is similar to that reported previously for ^{18}F-FAC.[11] Even though early ^{18}F-introduction gives a higher radiochemical yield, its automation is more difficult and the reliability and reproducibility is less easy to maintain. In addition, the radiochemical yield and overall radiosynthesis time of our methods might be further improvable using other synthesizers; alternatively, one could obtain the same amount of labelled nucleoside product by starting with a higher ^{18}F-activity. The reaction time for the radiolabelling step (20 min) is comparable with that used in the related ^{18}F-FMAU radiosynthesis,[12] reflective of the similar steric hindrance around the 2′-position in these nucleoside precursors. Shorter reaction times for this radiolabelling step were found to lead to lower yields of product through incomplete reaction.

Furthermore, it was shown that long reaction times and high reaction temperatures led to intramolecular anhydro formation identified by the detection of ^{18}F-FC. This study shows that rational precursor design can at least minimize the issue of side-product formation and hence can offer synthetic access of important PET radiotracer as a single stereoisomer. This method should be transferable to GMP environments as it offers a quick and reproducible two-step route towards ^{18}F-FAC comparable with the radiosynthesis of ^{18}F-FDG. However, further optimization is required in order to improve the radiochemical yield and prepare for transfer to production of clinical grade radiotracer.

Acknowledgements

This work was supported by Cancer Research Wales through PhD studentship funding (to J.-P. M.). We thank Dr Andrea Brancale (Cardiff University, School of Pharmacy and Pharmaceutical Sciences) for the advice and support with DFT calculations. We acknowledge the EPSRC National Mass Spectrometry Facility (Swansea, Wales, UK) for the provision of HR-MS determinations.

Conflict of Interest

The authors did not report any conflict of interest.

References

[1] J.-P. Meyer, K. C. Probst, A. D. Westwell, *J. Label. Compd. Radiopharm.* **2014**, *57*, 333–337.
[2] S. J. Martin, J. A. Eisenbarth, U. Wagner-Utermann, W. Mier, M. Henze, H. Pritzkow, U. Haberkorn, M. Eisenhut, *Nucl. Med. Biol.* **2002**, *29*, 263–273.
[3] A. F. Shields, *J. Nucl. Med.* **2003**, *44*, 1432–1434.
[4] M. Wagner, U. Seitz, A. Buck, B. Neumaier, S. Schultheiß, M. Bangerter, M. Bommer, F. Leithäuser, E. Wawra, G. Munzert, S. N. Reske, *Cancer Res.* **2003**, *63*, 2681–2687.
[5] R. E. Laing, M. A. Walter, D. O. Campbell, H. R. Herschman, N. Satyamurthy, M. E. Phelps, J. Czernin, O. N. Witte, C. G. Radu, *Proc. Natl. Acad. Sci. U. S. A.* **2009**, *106*, 2847–2852.
[6] J. T. Lee, D. O. Campbell, N. Satyamurthy, J. Czernin, C. G. Radu, *J. Nucl. Med.* **2012**, *53*, 275–280.
[7] C. G. Radu, C. J. Shu, E. Nair-Gill, S. M. Shelly, J. R. Barrio, N. Satyamurthy, M. E. Phelps, O. N. Witte, *Nat. Med.* **2008**, *14*(7), 783–788.
[8] O. S. Tehrani, O. Muzik, L. K. Heilbrun, K. A. Douglas, J. M. Lawhorn-Crews, H. Sun, T. J. Mangner, A. F. Shields, *J. Nucl. Med.* **2007**, *48*, 1436–1441.
[9] C.-Y. Wu, P.-C. Chan, W.-T. Chang, R.-S. Liu, M. M. Alauddin, H.-E. Wang, *Appl. Radiat. Isot.* **2009**, *67*, 1362–1365.
[10] N. Turkman, V. Paolillo, J. G. Gelovani, M. M. Alauddin, *Tetrahedron* **2012**, *68*, 10326–10332.
[11] M. Lazari, K. M. Quinn, S. B. Claggett, J. Collins, G. J. Shah, H. E. Herman, B. Maraglia, M. E. Phelps, M. D. Moore, R. M. van Dam, *EJNMMI Res.* **2013**, *3*, 52.
[12] N. Turkman, J. G. Gelovani, M. M. Alauddin, *J. Label. Compd. Radiopharm.* **2010**, *53*, 782–786.
[13] M. W. Schmidt, K. K. Baldridge, J. A. Boatz, S. T. Elbert, M. S. Gordon, J. H. Jensen, S. Koseki, N. Matsunaga, K. A. Nguyen, S. J. Su, T. L. Windus, M. Dupuis, J. A. Montgomery, *J. Comput. Chem.* **1993**, *14*, 1347–1363.
[14] C. Serra, C. Aragones, J. Bessa, J. Farras, J. Vilarrasa, *Tetrahedron Lett.* **1998**, *39*, 7575–7578.

Supporting Information

Additional supporting information may be found in the online version of this article at the publisher's web-site.